THE JOURNAL OF BIOLOGICAL CHEMISTRY
Vol. 278, No. 5, Issue of January 31, pp. 3055–3062, 2003
Printed in U.S.A.

Involvement of Tyrosines 114 and 139 of Subunit NuoB in the Proton Pathway around Cluster N2 in *Escherichia coli* NADH:Ubiquinone Oxidoreductase*

Received for publication, August 29, 2002, and in revised form, November 18, 2002
Published, JBC Papers in Press, November 20, 2002, DOI 10.1074/jbc.M208849200

Dirk Flemming‡§, Petra Hellwig§¶, and Thorsten Friedrich‡‖

From the ‡Institut für Org. Chemie und Biochemie, Albert-Ludwigs-Universität Freiburg, Albertstrasse 21, D-79104 Freiburg, Germany and the ¶Institut für Biophysik, Johann-Wolfgang-Goethe-Universität, Theodor-Stern-Kai 7, Haus 75, 60590 Frankfurt/M., Germany

The proton-pumping NADH:ubiquinone oxidoreductase (complex I) couples the transfer of electrons from NADH to ubiquinone with the translocation of protons across the membrane. Electron transfer is accomplished by FMN and a series of iron-sulfur clusters. Its coupling with proton translocation is not yet understood. Here, we report that the redox reaction of the FeS cluster N2 located on subunit NuoB of the *Escherichia coli* complex I induces a protonation/deprotonation of tyrosine side chains. Electrochemically induced FT-IR difference spectra revealed characteristic tyrosine signals at 1,515 and 1,498 cm^{-1} for the protonated and deprotonated form, respectively. Mutants of three conserved tyrosines on NuoB were generated by complementing a chromosomal in-frame deletion strain with *nuoB* on a plasmid. Though the single mutations did not alter the electron transport activity of complex I, the EPR signal of cluster N2 was slightly shifted. The tyrosine signals detected by FT-IR spectroscopy were roughly halved in the mutants Y114C and Y139C while only minor changes were detected in the Y154H mutant. The enzymatic activity of the Y114C/Y139F double mutant was 80% reduced, and FT-IR difference spectra of the double mutant revealed a complete loss the modes characteristic for protonation reactions of tyrosines. Therefore, we propose that tyrosines 114 and 139 on NuoB were protonated upon reduction of cluster N2 and were thus involved in the proton-transfer reaction coupled with its redox reaction.

The NADH:ubiquinone oxidoreductase, also known as respiratory complex I, links the electron transfer from NADH to ubiquinone with the translocation of protons across the membrane. By this means, complex I establishes a proton motive force required for energy consuming processes (1–3). Homologues of the complex are present in archaea, bacteria, and eukaryotes (4, 5). Complex I from bacteria generally consists of 14 different subunits (4–6). Seven of these are peripheral proteins including those subunits that bear all known redox groups of complex I, namely one FMN and up to nine iron-sulfur (FeS)[1] clusters. The remaining 7 subunits are hydrophobic proteins predicted to fold into 54 α-helices across the membrane (1, 2). They are most likely involved in ubiquinone reduction and proton translocation. The mitochondrial complex I of eukaryotes contains at least 29 extra proteins in addition to the homologues of the 14 prokaryotic complex I subunits (1, 2).

The genes of the *Escherichia coli* complex I are named *nuoA* to *nuoN* (7). *nuoC* and *D* are fused in *E. coli* giving rise to 13 different subunits assembling the complex (8). The preparation of the *E. coli* complex I contains one non-covalently bound FMN, two binuclear (N1a and N1b), and five tetranuclear (N2, N3, N4, N6a, and N6b) FeS clusters (Refs. 9, 10, and 11).[2] The tetranuclear cluster N5 present in complex I from other species has not yet been detected in this preparation. However, it should be present because of the preservation of the corresponding binding motif (7, 12, 13). The isolated complex can be split into a so-called NADH dehydrogenase fragment, a connecting fragment, and a membrane fragment (8, 9). The soluble NADH dehydrogenase fragment harbors the FMN and the EPR-detectable FeS clusters N1a, N1b, N3, and N4 (Refs. 9, 14, and 15).[2] The amphipathic connecting fragment contains the FeS clusters N2, N6a, and N6b (9, 11), while a chromophore with a yet unknown chemical structure, has been detected in the membrane fragment (16–18).

The so-called isopotential FeS clusters N1a, N1b, N3, N4, N6a, and N6b show similar midpoint potentials ranging from −0.28 to −0.24 mV. Together with the FMN ($E_{m,7}$ = −0.26 mV) they form the electron input part of complex I involved in NADH oxidation (4). Electrons are transferred further to the high potential cluster N2 ($E_{m,7}$ = −0.22 mV). Cluster N2 is located on NuoB (11, 19). This subunit contains solely three conserved cysteines as possible ligands (7). The fourth ligand of cluster N2, which may even reside on another subunit, remains to be established. The midpoint potential of FeS cluster N2 is, in contrast to most other clusters, pH-dependent (20). Therefore, it has been proposed that N2 is the electron donor to quinone and directly involved in proton translocation (13, 20).

If cluster N2 is involved in proton pumping, its redox reaction should be coupled to a protonation/deprotonation of the cluster itself and/or of surrounding amino acids. Recently, we were able to show that the reduction of N2 is coupled with a deprotonation of an Asp or Glu side chain by means of electrochemically induced FT-IR difference spectra (18, 21). In this study, we show that the reduction of cluster N2 is associated

* This work was supported by the Deutsche Forschungsgemeinschaft and the Fonds der Chemischen Industrie. The costs of publication of this article were defrayed in part by the payment of page charges. This article must therefore be hereby marked "*advertisement*" in accordance with 18 U.S.C. Section 1734 solely to indicate this fact.

§ Both authors contributed equally to this study.

‖ To whom correspondence should be addressed. Tel.: 49-(0)761-203-6060; Fax: 49-(0)761-203-6096; E-mail: tfriedri@uni-freiburg.de.

[1] The abbreviations used are: FeS, iron-sulfur; EPR, electron paramagnetic resonance; d-NADH, deamino-NADH; FT-IR, fourier-transform infrared; MES, 2-(*N*-morpholino)-ethanesulfonic acid; decylubiquinone, 2,3-dimethoxy-5-methyl-6-decylbenzoquinone; T, Tesla; WT, wild type.

[2] M. Uhlmann and T. Friedrich, unpublished data.

TABLE I
Oligonucleotides used for genomic amplification and site-directed mutagenesis
Underlined positions indicate new restriction sites, bold positions are responsible for the indicated mutation.

Oligonucleotide	Sequence
nuoB_for	5′-AATCTAGAGCTAATCGTCAACGCTAACC-3′
nuoB_rev	5′-AATCTAGAGCTAATCGTCAACGCTAACC-3′
nuoB Y114C_for	5′-CCGGTTATTCAGCGTCTG**TGT**GATCAGATGCTGG-3′
nuoB Y139C_for	5′-GGTGGTATGTACGATATC**TGT**TCCGTTGTGCAGGCG-3′
nuoB Y139_for	5′-GGTGGTATGTACGATATC**TTT**TCCGTTGTGCAGG-3′
nuoB Y154H_for	5′-ACATCCCGGGCTGCCGCGC-3′
nuoB Y154H_rev	5′-**GCAC**ATCAACCGGGATGAATTTATCGACGC-3′

with the protonation of two tyrosine side chains. Mutants of the three conserved tyrosines on NuoB were generated by complementation of a chromosomal *nuoB* deletion strain with expression of *nuoB* from a plasmid. Complementation of the *nuoB* deletion strain with either wild-type or mutated *nuoB* resulted in a fully assembled, active, and stable complex I. EPR spectroscopy of complex I isolated from the mutants revealed a shift in the signal of cluster N2. While the single mutants exhibited wild type NADH oxidase activity, the Y114C/Y139F double mutant showed an 80% reduced activity. FT-IR spectroscopy revealed that tyrosines 114 and 139 on NuoB are both involved in the protonation reaction coupled with the reduction of N2.

EXPERIMENTAL PROCEDURES

Materials and Strains—*E. coli* strains DH5α (22), AN387 (23), and ANN023[3] and the plasmids pSTBlue-1 (Novagen) and pBAD33 (24) were used. Strain ANN023 is a derivative of strain AN387 and contains a chromosomal in-frame deletion of *nuoB*. When required for maintenance of plasmids, chloramphenicol was added to 20 mg/liter and ampicillin to 100 mg/liter. All enzymes used for recombinant DNA techniques were from Roche Molecular Biochemicals. All other chemicals were from Merck (Darmstadt), Serva (Heidelberg), or Sigma.

Site-directed Mutagenesis and Expression of the nuoB Gene—*E. coli* genomic DNA was prepared with the Genomic DNA purification kit (MBI). The entire *nuoB* gene was amplified from *E. coli* genomic DNA as template and cloned into pSTBlue-1. Mutations in *nuoB* were created using either the QuickChange or ExSite PCR-based site-directed mutagenesis kit (both from Stratagene) and are given in Table I. Sequences of all plasmids were confirmed by DNA sequencing. pSTBlue-1 containing *nuoB* was digested with *Kpn*I/*Sac*I, and the resulting 860-bp fragment was cloned into the expression vector pBAD33. The resulting plasmids were named pBAD-B^{type} with *type* defining either the wild type gene or the corresponding mutation. The plasmids carrying the mutation were used for transformation of the deletion strain ANN023. Transformants were grown in a 10-liter culture of LB medium at 37 °C. Arabinose was added to a final concentration of 0.2% (w/v) at an OD_{600} of approximate 0.5. Three hours after induction, 30–40 g of cells were harvested by centrifugation for 10 min at 4,000 × *g*. Cells were washed with 50 mM MES/NaOH, pH 6.0 and stored at −80 °C.

Isolation of Complex I from NuoB Mutants—In principle, complex I was isolated by means of a procedure developed for a strain overproducing complex I (10). However, the membranes of the mutant strains were not washed with NaBr to remove ATP synthase as described due to the lower amount of complex I. Therefore, the preparations contained detectable amounts of ATP synthase, which, however, did not interfere with our assays. All steps were carried out at 4 °C. 60 g of cells were resuspended in 150 ml of 50 mM MES/NaOH, 0.1 mM phenylmethanesulfonyl fluoride, pH 6.0, with 10 μg/ml DNase I and disrupted by a single pass through a French Pressure cell (SLM Aminco) at 110 MPa. Cell debris was removed by centrifugation for 20 min at 36,000 × *g*, and cytoplasmic membranes were obtained by centrifugation for 1 h at 250,000 × *g*. Membrane proteins were extracted by adding dodecyl maltoside to a final concentration of 3%. The solution was gently homogenized and centrifuged for 1 h at 250,000 × *g*. The supernatant was applied to a 60-ml Source 15Q (Amersham Biosciences) column equilibrated in 50 mM MES/NaOH, 50 mM NaCl, and 0.1% dodecyl maltoside, pH 6.0. The column was eluted with a 700-ml linear gradient of 50–350 mM NaCl in 50 mM MES/NaOH, 0.1% dodecyl maltoside, pH 6.0 at a flow rate of 4 ml/min. Fractions containing NADH/ferricyanide reductase activity were combined, concentrated by precipitation with 9% (w/v; final concentration) polyethylene glycol 4,000 and dissolved in 2 ml of 50 mM MES/NaOH, 50 mM NaCl, and 0.1% dodecyl maltoside, pH 6.0. The protein was subjected to size-exclusion chromatography on a 180-ml Ultrogel AcA 34 (Serva) column in 50 mM MES/NaOH, 50 mM NaCl, and 0.1% dodecyl maltoside, pH 6.0, at a flow rate of 7 ml/h. Peak fractions were pooled and applied to a 10- ml Source 15Q (Amersham Biosciences) equilibrated as described above and eluted with a 100-ml linear gradient of 50–350 mM NaCl in the same buffer at a flow rate of 2 ml/min. Fractions with NADH/ferricyanide reductase activity were pooled and stored at −80 °C. Complex I from wild type was prepared with the same procedure. The NADH dehydrogenase fragment of the complex was isolated as described (15). For electrochemistry, the preparations were concentrated by ultrafiltration (Centricon 100, Amicon) to ~0.2 mM.

Electrochemistry—The ultrathin layer spectroelectrochemical cell for UV/Vis and IR was used as previously described (25). Sufficient transmission in the 1,800 cm^{-1} to 1,000 cm^{-1} range, even in the region of strong water absorbance around 1,645 cm^{-1}, was achieved with the cell pathlength set to 6–8 μm. To avoid protein denaturation, the gold grid-working electrode was chemically modified by a 2 mM cysteamine solution as reported (25). In order to accelerate the redox reaction, the following mediators were used at a final concentration of 45 μM each: ferrocenyltrimethylammoniumiodide (+645 mV), 1,1′-dicarboxylferrocene (+644 mV), diethyl-3-methylparaphenylenediamine (+367 mV), ferricyanide (+424 mV), dimethylparaphenylenediamine (+371 mV), 1,1′-dimethylferrocene (+341 mV), tetramethylparaphenylenediamine (+270 mV), tetrachlorobenzoquinone (+280 mV), 2,6-dichlorophenolindophenol (+217 mV), ruthenium hexamine chloride (200 mV), 1,2-naphthoquinone (−145 mV), trimethylhydroquinone (100 mV), menadione (−12 mV), 2-hydroxy-1,4-naphtoquinone (−125 mV), anthraquinone-2-sulfonate (−225 mV), neutral red (−307 mV), benzyl viologen (−360 mV), and methyl viologen (−446 mV). At the given concentrations and with the pathlength below 10 μm, no spectral contributions from the mediators in the visible and IR range used were detected in control experiments with samples lacking the protein. Approximately 6–7 μl of the protein solution were sufficient to fill the spectroelectrochemical cell.

FT-IR Spectroscopy—FT-IR difference spectra as a function of the applied potential were obtained simultaneously from the same sample with a setup combining an IR beam from the interferometer (modified IFS 25, Bruker, Germany) for the 4,000 cm^{-1} to 1,000 cm^{-1} range and a dispersive spectrometer for the 400–900-nm range as reported previously (26, 27). First, the protein was equilibrated with an initial potential at the electrode and single beam spectra in the visible and IR range were recorded. Then a potential step toward the final potential was applied and single beam spectra of this state were again recorded after equilibration. Difference spectra were calculated from the two single beam spectra with the initial single beam spectrum taken as reference. No smoothing or deconvolution procedures were applied. The equilibration process for each applied potential was followed by monitoring the electrode current and by successively recording spectra in the visible range until no further changes were observed. The equilibration generally took less than 8 min for the full potential step from −0.5 V to 0.0 V. Typically, 128 interferograms at 4 cm^{-1} resolution were coadded for each single beam IR spectrum and Fourier-transformed using triangular apodization. Up to 5 × 20 difference spectra have been averaged. The presence of atmospheric water vapor was avoided as described (21).

EPR Spectroscopy—Low temperature EPR measurements were conducted with a Bruker EMX 1/6 spectrometer. The sample temperature was controlled with an Oxford Instruments ESR-9 helium flow cryostat. Complex I at 10 mg/ml was reduced with a 1,000-fold molar excess of NADH in the presence of redox mediators as described (9). The EPR

[3] V. Spehr, T. Bischof, and T. Friedrich, unpublished results.

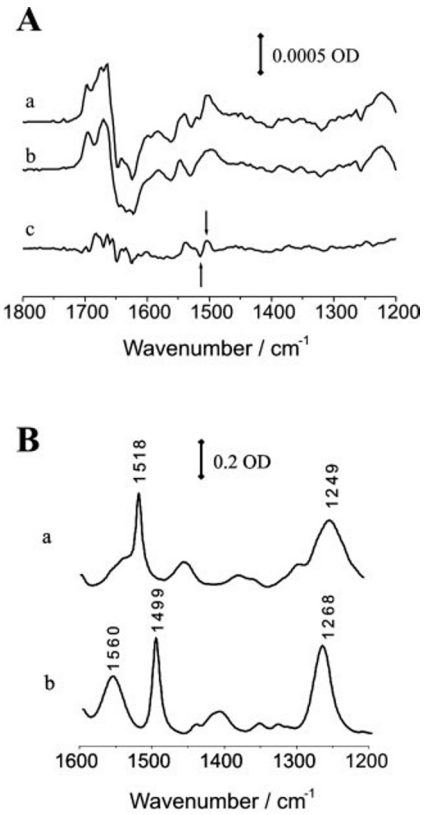

FIG. 1. **FT-IR spectroscopic detection of tyrosine residues involved in the redox reaction of complex I.** *A*, oxidized − reduced difference FT-IR spectra of complex I (*a*), the NADH dehydrogenase fragment of complex I (*b*), both for the potential step from −0.5 to 0.0 V, and double difference FT-IR spectra of the difference spectra of complex I minus the difference spectra of NADH dehydrogenase fragment (*c*). *B*, absorbance spectra of tyrosine (Fluka) *in situ* protonated upon solution in 1 M HCl (*a*) and deprotonated upon solution in 1 M NaOH (*b*). The contributions of the solvent were interactively subtracted. The signals at 1,515 and 1,498 cm^{-1} discussed to specifically indicate the protonation/deprotonation of tyrosine side chain(s) are marked with *arrows*.

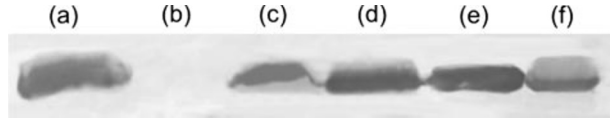

FIG. 2. **Western blot of membranes of the *E. coli* strains AN387 (*a*), ANN023 (*b*), ANN023/pBAD33-B^{WT} (*c*), ANN023/pBAD33-B^{Y114C} (*d*), ANN023/pBAD33-$B^{Y114C/Y139F}$ (*e*), and of complex I isolated from strain ANN023/pBAD33-B^{Y114C} (*f*).** Western blotting was performed with an antiserum raised against NuoB.

tube was frozen in 5:1 isopentane/methylcyclohexane (v/v) at 150 K. The magnetic field was calibrated using a strong pitch standard.

Enzyme Activity—The NADH:decylubiquinone reductase activity of complex I was measured with a Perkin Elmer 156 dual-wavelength spectrophotometer using the wavelength 340 and 400 nm and ϵ of 6.3 mM^{-1} cm^{-1}. The assay contained 5 mM MES/NaOH, 0.1 mM NaCl, pH 6.0, and 50 μM NADH and 25 μM decylubiquinone. The reaction was started by addition of 10 μg of complex I (28). The NADH/ferricyanide reductase activity, and the NADH oxidase activity were measured as described (29, 30).

Other Analytical Procedures—Protein concentration was measured with the biuret method using bovine serum albumin as standard. Sucrose gradient centrifugation in the presence of 0.2% dodecyl maltoside was performed as described (9). Following SDS-PAGE protein bands were either stained with Coomassie Blue or electroblotted onto 0.45-μm pore size nitrocellulose membrane (Schleicher und Schüll) according to Ref. 31. A rabbit polyclonal antibody raised against NuoB was used for detection.

RESULTS

FT-IR Spectroscopy of Wild Type Complex I—Electrochemically-induced FT-IR difference spectra of complex I contain contributions from redox-dependent changes in the protein structure and protonation states of cofactors and individual amino acids. In order to detect changes associated with the redox reaction of FeS cluster N2 we recorded FT-IR spectra of complex I at the potential step from −0.5 to 0.0 V (Fig. 1*A*, *a*). The difference spectrum of complex I obtained for this potential step was compared with difference spectra of the NADH dehydrogenase fragment of complex I for the same potential step (Fig. 1*A*, *b*).

The double difference spectrum (Fig. 1*A*, *c*) showed spectral contributions from rearrangement of the polypeptide backbone and contributions of individual amino acids such as the protonation/deprotonation of aspartic or glutamic side chain(s) as reported (21). In addition, the spectrum showed contributions at 1,515 and 1,500 cm^{-1}, which were tentatively attributed to tyrosine side chains. From model spectra of the protonated tyrosine (Fig. 1*B*, *a*) the prominent signal at 1,518 cm^{-1} was attributed to the ν_{19}(CC) ring mode. At 1,249 cm^{-1} a signal composed of the $\nu_{7'a}$(CO) vibration and the δ(COH) vibration was expected, the position being sensitive to the hydrogen-bonding environment. For deprotonated tyrosine in solution (Fig. 1*B*, *b*) the $\nu_{8a}/_{8b}$(CC) ring mode was identified at 1,560 cm^{-1} and the ν_{19}(CC) ring mode at 1,499 cm^{-1}, thus reflecting the sensitivity of the ring modes to the protonation state of the phenol group. The $\nu_{7'a}$(CO) mode was present at 1,269 cm^{-1} (32–35). From direct comparison of the signals in the double difference spectrum and in the model compound spectra, a protonation of one or more tyrosine side chains was suggested to be coupled with the reduction of the enzyme. We set out to confirm this tentative assignment by site-directed mutagenesis of the conserved tyrosines on NuoB.

Complementation of the nuoB Deletion—Approximately 70% of *nuoB* was deleted from the chromosome of wild type strain AN387 without interrupting the reading frame.[3] The resulting strain ANN023 was complemented with the wild type *nuoB* on the plasmid pBAD33, under control of the inducible pBAD promotor. This strain was called ANN023/pBAD33-B^{WT}.

The presence of NuoB in the strains AN387, ANN023, and ANN023/pBAD33-B^{WT} was determined by reaction of a specific antibody with blotted membrane proteins after SDS-PAGE (Fig. 2). NuoB was detected in the membranes of the strains AN387 and ANN023/pBAD33-B^{WT} while it was missing in the membranes of strain ANN023.

We tested whether NuoB expressed from the plasmid was able to assemble an intact complex I with the residual complex I subunits encoded on the chromosome by sucrose gradient centrifugation (Fig. 3). Dodecyl maltoside extracts of cytoplasmic membranes from strains ANN023 and ANN023/pBAD33-B^{WT} were applied on a 12-ml sucrose gradient. Complex I from *E. coli* typically sediments two thirds of the way through the gradient as detected by its NADH/ferricyanide activity (9, 10). No NADH/ferricyanide activity was detectable in the corresponding fractions of strain ANN023 indicating that complex I was not assembled in the absence of NuoB (Fig. 3). Instead, fractions in the first third of the gradient exhibited NADH/ferricyanide activity, which stemmed from the alternative, non-proton pumping NADH dehydrogenase. The expression of this alternative NADH dehydrogenase is increased in the absence of complex I. The sedimentation profile of the extract obtained from strain ANN023/pBAD33-B^{WT} showed NADH/ferricyanide activity in the fractions corresponding to the wild type enzyme (Fig. 3). Western blot analysis confirmed the presence of NuoB in the corresponding fractions (data not shown). Again, the

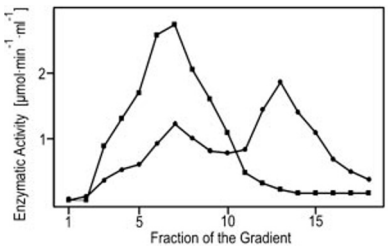

FIG. 3. **Sucrose gradient centrifugation of detergent extracts of cytoplasmic membranes of strains ANN023 (*closed squares*) and ANN023/pBAD-B^{WT} (*closed circles*).** Cytoplasmic membranes were extracted with 3% dodecyl maltoside (w/v) and separated by means of gradients of 5–25% (w/v) sucrose in 50 mM MES/NaOH, pH 6.0, 50 mM NaCl, and 0.2% dodecyl maltoside. Each gradient was loaded with 4 mg of protein. Fractions of the gradients (numbered 1–18 from *top* to *bottom*) were collected and analyzed for NADH/ferricyanide reductase activity.

alternative NADH dehydrogenase was detected in the first third of the gradient but in smaller amounts. These data showed that the assembly of complex I was restored by complementation of *nuoB* on a plasmid.

The amount of complex I in the cytoplasmic membranes of these strains was estimated from the (d-) NADH/ferricyanide activity as well as from the (d-) NADH oxidase activity (Table 2). The artificial substrate d-NADH was used to discriminate the two membrane-bound NADH dehydrogenases of *E. coli* (30, 36). While NADH can be used by both NADH dehydrogenases, d-NADH preferently reacts with complex I. The d-NADH/ferricyanide activity as well as the d-NADH oxidase activity was nearly abolished in strain ANN023 lacking an assembled complex I. These activities were restored to wild type level in strain ANN023/pBAD33-B^{WT} (Table 2). The NADH/ferricyanide and NADH oxidase activity of strain ANN023 was decreased to about one-third of the wild type activity due to that of the alternative NADH dehydrogenase. Two-thirds of the NADH oxidase activity was inhibited by 10 μM piericidin A in AN387 and ANN023/pBAD33-*B*^{WT}. The NADH oxidase activity of strain ANN023 was virtually not inhibited by piericidin A, demonstrating the lack of complex I in this strain.

Site-directed Mutagenesis of nuoB—Among all subunits present in complex I from different sources, NuoB shows the highest degree of sequence conservation (4, 7). Alignment of the homologues of NuoB showed the presence of three tyrosine residues being conserved within all three domains of life (Fig. 4).

Involvement of the conserved tyrosines in the protonation/deprotonation induced by the redox reaction of cluster N2 was advanced by constructing site-directed mutants. The mutants Y114C, Y139C, Y154H, and Y114C/Y139F of NuoB were expressed using the system described above. To determine whether complex I was assembled in the mutant strains, the (d-) NADH/ferricyanide reductase activity and the (d-) NADH oxidase activity of cytoplasmic membranes were measured as described above. The strains carrying a single mutation exhibited activities with d-NADH as substrate comparable to the wild type strain AN387 and the complemented strain ANN023/pBAD33-B^{WT} (Table 2) indicating that complex I in the mutants was able to transfer electrons from NADH to ubiquinone. The NADH oxidase activity in these mutant strains was inhibited by about two-thirds by 10 μM piericidin A. Thus, the amount and the activity of complex I in the membranes was not influenced by the mutations introduced. The d-NADH/ferricyanide activity of the strain carrying the Y114C/Y139F double mutation was 50% reduced compared with wild type and this strain showed 20% of the d-NADH oxidase activity. NuoB was detected in the cytoplasmic membranes from this mutants by Western blot analysis (Fig. 2). These data suggested that half of the amount of complex I with a strongly reduced activity is present in this strain.

Isolation of Complex I from the Mutant Strains—For spectroscopic characterization complex I was isolated from the mutants Y114C, Y139C, Y154H, and Y114C/Y139F. All steps were performed in the presence of 0.1% dodecyl maltoside at pH 6.0. As an example, the preparation of the complex from the mutant Y114C is shown in Fig. 5. The other preparations showed similar elution profiles. The enzyme eluted from both anion-exchange chromatography on Source Q-15 at 280 mM NaCl and from the Ultrogel AcA34 size-exclusion column at 70 ml (Fig. 5). Thus, the mutant complexes showed chromatographic properties comparable to the wild type complex (10). Approximately 1–2 mg of complex I were obtained from 60 mg of cells of the single mutant strains (Table 3), while less than 1 mg was obtained from the double mutant strain.

Upon SDS/PAGE the preparation was resolved into the 13 complex I subunits plus some protein bands due to the presence of ATP synthase (Fig. 5). The presence of NuoB in the preparations was confirmed by Western blot analysis (Fig. 2). Complex I isolated from the single mutants catalyzed electron transfer from NADH to ubiquinone with a rate of 2.1–2.3 μmol of NADH/min·mg in the presence of 50 μM NADH and 25 μM decylubiquinone. Complex I isolated from the Y114C/Y139F double mutant showed no NADH:decylubiquinone activity. Under the same conditions the wild type exhibits an activity of 2.4 μmol of NADH/min·mg.

EPR Spectroscopic Analysis of the NuoB Mutants—NuoB contains three conserved cysteines which are *bona fide* ligands of cluster N2 (8, 14, 37). The fourth ligand is not yet known. To investigate whether one of the conserved tyrosines is the missing fourth ligand, we determined the amount and spectral properties of the FeS clusters in complex I by EPR-spectroscopy. The samples were reduced by an excess NADH in the presence of redox mediators. The EPR spectra recorded at 40 K were nearly identical, indicating no changes in the microenvironment of the binuclear FeS clusters N1a and N1b (data not shown). The spectra recorded at 13 K revealed the presence of the EPR-detectable clusters N2, N3, and N4 (Fig. 6). The amount of cluster N2 measured as signal amplitude was diminished by about one-fifth in all single mutants. A small but clear shift of the g_z signal of N2 from 2.049 in the wild type to 2.051 in the mutant Y154H and to 2.052 in the mutants Y114C and Y139C was detected (Fig. 6). The $g_{x,y}$ signal of N2 did not change. The EPR spectrum from the double mutant Y114C/Y139F showed no change in the g_z signal of N2 with respect to its spectral position and amplitude. However, its $g_{x,y}$ signal was decreased by ~50% (Fig. 6) This spectral region was hard to evaluate due to the spectral overlap with signals from cluster N3 and N4. From these data it was evident that neither of the three tyrosines was a ligand of cluster N2, but that they were in close vicinity.

FT-IR Spectroscopic Analysis of the NuoB Mutants—The possible participation of the conserved tyrosines in the proton pathway coupled with the redox reaction of cluster N2 was investigated by means of FT-IR spectroscopy (21). FT-IR spectra of the isolated complexes were recorded in an electrochemical cell for the potential step from −0.5 to 0.0 V (Fig. 7*A*). Complex I isolated from the mutant strains was more unstable during the electrochemical measurements than the complex from wild type. This resulted in a lower signal to noise ratio of the corresponding spectra. Whereas the difference spectra of the Y154H mutant revealed only small vari-

TABLE II
Enzyme activities of the membrane-bound NADH dehydrogenases of E. coli wild type and various NuoB mutants

Strain	NADH/ferricyanide reductase activity	d-NADH/ferricyanide reductase activity	NADH oxidase activity	d-NADH oxidase activity	Inhibition of the NADH oxidase activity by piericidin A
		μmol min^{-1} mg^{-1}			%
AN387 (wild type)	1.0	0.8	0.15	0.06	69
ANN023 (ΔnuoB)	0.6	0.1	0.05	0	<10
ANN023/pBAD-B^{WT}	0.9	0.8	0.08	0.05	67
ANN023/pBAD-B^{Y114C}	0.9	0.8	0.07	0.05	66
ANN023/pBAD-B^{Y139C}	0.8	0.8	0.08	0.04	65
ANN023/pBAD-B^{Y154H}	0.9	0.7	0.08	0.05	67
ANN023/pBAD-B$^{Y114C/Y139F}$	0.5	0.4	0.05	0.01	<10

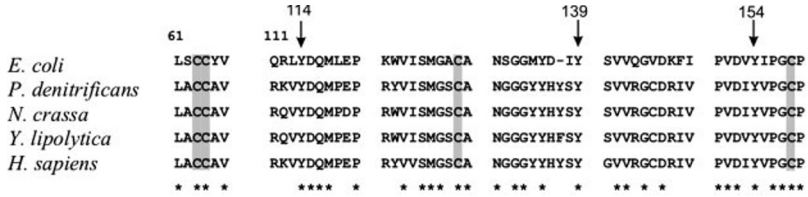

FIG. 4. **Sequence alignment of NuoB homologues.** The protein sequences from various organisms were aligned using ClustalX (44). Identical amino acids are marked by *asterisks*. Conserved cysteines are shaded in *gray*, the position of the conserved tyrosines are marked with *arrows* (*E. coli* numbering).

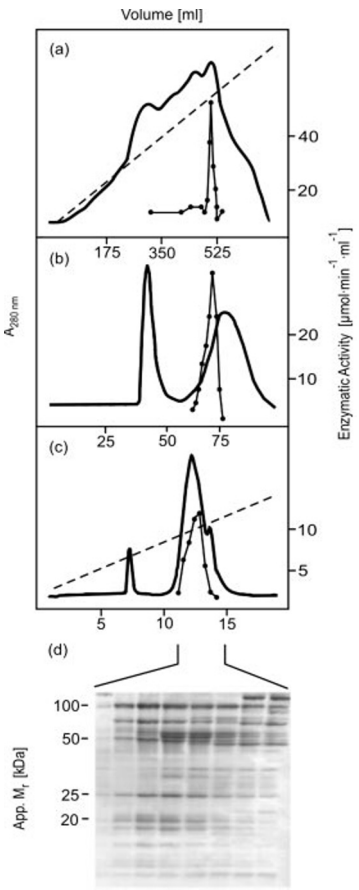

FIG. 5. **Isolation of *E. coli* complex I from strain ANN023/pBAD-B^{Y114C}.** Chromatography on Source 15Q (*a*); chromatography on Ultrogel AcA 34 (*b*); chromatography on Source 15Q (*c*); absorbance at 280 nm (−); NADH/ferricyanide reductase activity (●); NaCl gradient (−). SDS/PAGE of the indicated fractions of the second anion exchange chromatography (*d*).

ations in comparison to wild type spectra, strong variations were evident for the Y114C, Y139C, and Y114C/Y139F mutants in the amide I range, where the contributions of the polypeptide backbone are included. These shifts indicated structural rearrangement of the protein upon mutation of the tyrosine residues in NuoB. In addition, smaller variations for the full spectral range were seen.

In order to depict possible variations of the modes typical for the tyrosine residues, double difference spectra were obtained for the critical spectral range from 1,530 to 1,480 cm^{-1}, by subtracting the spectra of the mutant enzymes from the corresponding spectra of the NADH dehydrogenase fragment (Fig. 7*B*). The absoption of the tyrosine residues proved to be located as shoulders of a positive peak at 1,506 cm^{-1} in complex I (Fig. 7*B*).

The difference spectra of wild type complex I displayed a prominent signal at 1,515 cm^{-1}, which we interpreted as the protonation of one or more tyrosine residues due to the reduction of cluster N2 as well as the mode at 1,498 cm^{-1}, which we interpreted as the deprotonation of the corresponding tyrosine side chain(s) due to the oxidation of cluster N2 (Figs. 1 and 7). The decrease of both signals observed for the mutant Y154H was significantly smaller from the extinction coefficients observed in model compound spectra than expected. This excluded tyrosine side chain 154 to be addressed by the redox reaction. The introduced mutation might have an influence on nearby residues or the involvement of low amide II signals. The strongest decrease of the modes at 1,515 and 1,498 cm^{-1} were observed for the Y114C and Y139C mutants. The amplitude of the signal was roughly halved in both mutants, demonstrating that Y114 and Y139 were protonated upon reduction of cluster N2. A residual signal of the characteristic tyrosine modes accounting for another tyrosine residue was present in both single mutants suggesting that no other tyrosines were involved in the signals discussed here. This conclusion was supported by the electrochemically induced FT-IR difference spectra of the double mutant Y114C/Y139F. Clearly any signal that was attributed to the tyrosines was absent.

DISCUSSION

Knowledge of the mechanism of complex I is rather limited due to its enormous complexity in combination with the lack of structural data. The mitochondrial complex I is made up of at least 43 different subunits (38) with seven of them being encoded on the mitochondrial genome. Together these subunits constitute a molecular mass of about 1 MDa (1, 2). Although the bacterial complex shows a simpler composition of 14 different subunits, this number is still quite large (4–6, 39). In addition,

TABLE III
Isolation of E. coli complex I from strain ANN023/pBAD33-B^{Y114C}

	Volume	Protein[a]	NADH/ferricyanide reductase activity		Yield
			Total	Specific	
	mL	*mg*	*μmol min^{-1}*	*μmol min^{-1} mg^{-1}*	*%*
Membranes	40	2200	2400	1.1	100
Extract	35	1300	2100	1.6	88
Source 15Q	45	120	970	8	40
AcA 34	9	7	90	13	3.7
Source 15Q	2	1	40	40	1.6

[a] The preparation was started from 60 g of wet cells.

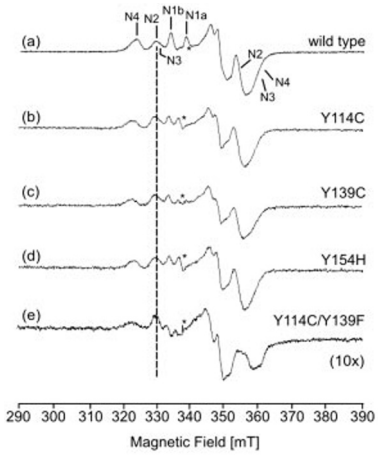

FIG. 6. **EPR spectra of complex I isolated from wild type (*a*) and the mutants Y114C (*b*), Y139C (*c*), Y154H (*d*), and Y114C/Y139F (*e*).** The spectra were recorded at 13 K and 5 milliwatts. The signals of the FeS clusters N1a, N1b, N2, N3, and N4 are indicated. The position of the g_z signal of cluster N2 is indicated by the *dotted line* for a better comparison. The *asterisks* denote the radical signal of the redox mediators. Other EPR conditions were: microwave frequency, 9.44 GHz; modulation amplitude, 0.6 mT; time constant, 0.124 s; scan rate, 17.9 mT/min.

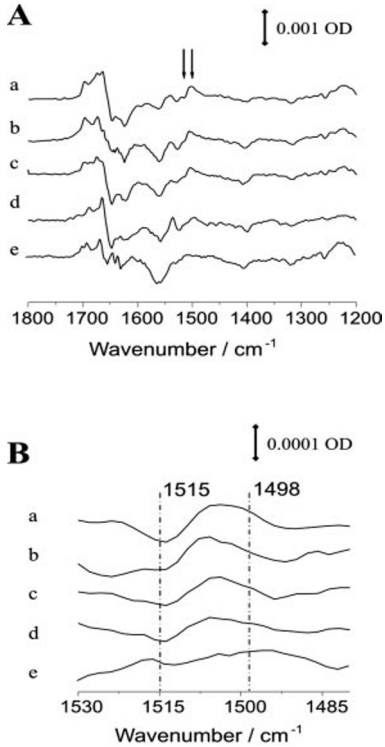

FIG. 7. **FT-IR difference spectra of complex I from wild type and NuoB mutants for the potential step from −0.5 to 0.0 V.** *A*, difference spectrum of oxidized − reduced spectra of complex I isolated from wild type (*a*), ANN023/pBAD-B^{Y139C} (*b*), ANN023/pBAD-B^{Y154H} (*c*), ANN023/pBAD-B^{Y114C} (*d*), and ANN023/pBAD-B$^{Y114C/Y139F}$. *B*, double difference spectra of difference spectra of complex I minus difference spectra of NADH dehydrogenase fragment. The designation of the spectra is the same as in *A*. An enlargement of the spectral region from 1,530 to 1,480 cm^{-1} is shown. The absorptions of the tyrosine side chains are marked with *dotted lines*.

mutagenesis of individual subunits turned out to be very laborious as they have to be introduced as unmarked mutations in the chromosome. Insertion of a resistance cartridge in the *nuo* operon coding the complex I subunits disturbed the assembly of the complex.[4] So far, an easy to manage extrachromosomal system containing the 16-kb *nuo*-operon is not available. Therefore, we constructed a strain with an in-frame deletion of the complex I gene of interest, namely *nuoB*. The mutant ANN023 is devoid of 70% of the *nuoB* reading frame. Neither NuoB nor a smaller fragment of it was detected in the strain ANN023 (Fig. 2). The absence of NuoB was sufficient to prohibit the assembly of the entire complex as the membranes of strain ANN023 did not exhibit any d-NADH oxidase activity and a strongly reduced d-NADH/ferricyanide activity (Table 2). When the cells were supplied with *nuoB* on the pBAD33 expression plasmid, complex I was rescued (Table 2). The amount of complex I in membranes was restored to 90% compared with the wild type as judged by the d-NADH oxidase activity and the specific d-NADH/ferricyanide reductase activity of cytoplasmic membranes (Table 2), as well as by the specific NADH/ferricyanide reductase activity of the membrane extract after sucrose gradient centrifugation (Fig. 3). Using this system we were able to introduce point mutations in NuoB and to investigate the participation of individual amino acids in proton translocation of complex I.

The FeS cluster N2 is located on NuoB as indicated by site-directed mutagenesis of complex I from *E. coli*, *Yarrowia lypolytica*, and *Neurospora crassa* (8, 19, 37). Although N2 is a tetranuclear FeS cluster, NuoB lacks a canonical motif for the coordination of such a cluster (7, 12, 13). Two of four of the conserved cysteines on NuoB are located in the vicinity. Although it cannot be excluded, it is unlikely that both cysteines are ligands to the same cluster. The fourth ligand of this cluster remains to be detected. Here, we detected that the reduction of cluster N2 was linked with the protonation of tyrosine residues (Fig. 1). It could be possible that one of these tyrosine residues is the fourth ligand of N2. EPR spectra of complex I isolated from the NuoB tyrosine mutants showed the presence of N2 in almost the same amount as in the wild type (Fig. 6). Complex I isolated from the mutants showed a shift of the signals of N2 (Fig. 6). However, the change from a tyrosine to a cysteine, phenylalanine, or histidine ligand would have caused a more severe change of the cluster signal or even a loss of the cluster as it has been reported for the *E. coli* and the *N. crassa* complex (8, 19). Therefore, the tyrosine residues on NuoB investigated in this study were located close to but did not ligate N2.

[4] A. Berger, V. Spehr, and T. Friedrich, unpublished results.

The mutations of the conserved tyrosine residues resulted in minor structural rearrangements of the protein backbone. This was evident from the enzymatic activity, which was close to wild type level (Table 2) as well as from the EPR and FT-IR spectra (Figs. 6 and 7). These were the only effects detected in the mutant Y154H (and Y154F, data not shown). However, irrespective of the general changes in the spectra, the tyrosine signals at 1,515 and 1,498 cm^{-1} of complex I isolated from strains Y114C and Y139C were approximately halved in each mutant and absent in the double mutant (Fig. 7). Our data implied that tyrosine residues 114 and 139 of NuoB were part of the proton pathway coupled with the redox reaction of cluster N2. It is noteworthy that the structural rearrangements upon electron transfer reported for the wild type enzyme (21) were strongly reduced in the Y114C/Y139F double mutant (Fig. 7). The proton pump mechanism of complex I might be coupled to conformational changes of the complex (6, 28). The loss of the conformational flexibility of the complex from the double tyrosine mutant is in line with the possible involvement of the two tyrosine residues in proton pumping.

The redox driven proton pump within complex I is suggested to be linked with the redox reaction of cluster N2 due to pH dependence of its midpoint potential (20). The pH dependence of N2 exhibits a slope of −60 mV/pH (20) implying that the redox Bohr group associated with N2 receives a proton in the reduced state and becomes deprotonated with the oxidation of N2. The protonation/deprotonation of tyrosine residues 114 and 139 of NuoB were coupled with the redox reaction of N2 in such a way that they might be discussed for such a redox Bohr group. However, the electron transport activity of the complex from the single mutants was comparable to the one of the wild type demonstrating an uncoupling of electron transfer involving N2 and protonation of the tyrosine residues. Thus, the individual tyrosine residues 114 and 139 on NuoB cannot represent the redox Bohr group associated with N2. However, complex I of the Y114C/Y139F double mutant exhibited only 20% of the wild type d-NADH oxidase activity in the membrane (Table 2), and the isolated complex had no enzymatic activity. This implies the presence of a cluster of protonable groups including tyrosine residues 114 and 139 that sense the redox state of cluster N2.

It is not unusual that a single mutation within a proton pathway does not correlate with a loss of electron transfer activity. Previous detailed studies of other proton pumping enzymes such as cytochrome *c* oxidase showed this effect. There are two possible explanations for this phenomenon. First, the electron transfer may be uncoupled from the proton translocation and second, single mutations in a large proton pathway do not affect turnover (Refs. 40 and 42 and references within). Double or triple mutants are needed in the latter case for a complete inhibition of coupled electron/proton transfer. This was demonstrated for example in the case of the highly conserved arginine side chains bridging the propionates of hemes *a*/*b* and a_3/o_3, respectively, in cytochrome oxidase from different organisms (42, 43) as well as by several residues forming the D-path of cytochrome oxidase (40, 41). Our study could represent another example where the mutation of both tyrosine residues is needed to influence the enzymatic activity.

Mutations from a tyrosine residue to a cysteine, phenylalanine, and histidine residue, as presented here, still allow hydrogen bonding to be established. Therefore, it would still be possible to transfer protons in a large proton path as found for example in cytochrome oxidase. We note that a deletion of a putative hydrogen bonding would have induced strong but nonspecific structural variations. This would have prohibited a discussion of the spectroscopic data.

As a working hypothesis we speculate that tyrosine residues 114 and 139 on NuoB are protonated upon reduction of N2. The proton being released from the tyrosine residues upon oxidation of N2 is transferred via yet unknown groups to an acidic amino acid on NuoB, which is subsequently protonated (21). Thus, the redox reaction of cluster N2 would be linked with the uptake of protons by tyrosine residues and a release of protons to an acidic amino acid. This could initiate a directed proton movement given the right spatial orientation of the tyrosine residues and the acidic amino acid(s) around cluster N2.

Acknowlegments—We thank Helga Lay and Franz Butz for excellent technical assistance, Stefan Stolpe for help in enzyme preparation, and Linda Böhm for help in preparing the manuscript.

REFERENCES

1. Weiss, H., Friedrich, T., Hofhaus, G., and Preis, D. (1991) *Eur. J. Biochem.,* **197,** 563–576
2. Walker, J. E. (1992) *Quart. Rev. Biophys.*, **25,** 253–324
3. Brandt, U. (1997) *Biochim. Biophys. Acta* **1318,** 79–91
4. Friedrich, T., Steinmüller, K., and Weiss, H. (1995) *FEBS Lett.* **367,** 107–111
5. Friedrich, T., and Scheide, D. (2000) *FEBS Lett.* **479,** 1–5
6. Friedrich, T. (2001) *J. Bioenerget. Biomembr.* **33,** 169–179
7. Weidner, U., Geier, S., Ptock, A., Friedrich, T., Leif, H., and Weiss, H. (1993) *J. Mol. Biol.* **233,** 109–122
8. Friedrich, T. (1998) *Biochim. Biophys. Acta* **1364,** 134–146
9. Leif, H., Sled, V. D., Ohnishi, T., Weiss, H., and Friedrich, T. (1995) *Eur. J. Biochem.* **230,** 538–548
10. Spehr, V., Schlitt, A., Scheide, D., Guénebaut, V., and Friedrich, T. (1999) *Biochemistry* **38,** 16261–16267
11. Rasmussen, T., Scheide, D., Brors, B., Kintscher, L., Weiss, H., and Friedrich, T. (2001) *Biochemistry* **40,** 6124–6131
12. Yano, T., Magnitsky, S., and Ohnishi, T. (2000) *Biochim. Biophys. Acta* **1459,** 299–305
13. Ohnishi, T. (1998) *Biochim. Biophys. Acta* **1364,** 186–206
14. Braun, M., Bungert, S., and Friedrich, T. (1998) *Biochemistry* **37,** 1861–1867
15. Bungert, S., Krafft, B., Schlesinger, R., and Friedrich, T. (1999) *FEBS Lett.* **460,** 207–211
16. Schulte, U., Haupt, V., Abelmann, A., Fecke, W., Brors, B., Rasmussen, T., Friedrich, T., and Weiss, H. (1999) *J. Mol. Biol.* **292,** 569–580
17. Friedrich, T., Abelmann, A., Brors, B., Guénebaut, V., Kintscher, L., Leonard, K., Rasmussen, T., Scheide, D., Schlitt, A., Schulte, U., and Weiss, H. (1998) *Biochim. Biophys. Acta* **1365,** 215–219
18. Friedrich, T., Brors, B., Hellwig, P., Kintscher, L., Scheide, D., Schulte, U., Rasmussen, T., Mäntele, W., and Weiss, H. (2000) *Biochim. Biophys. Acta* **1459,** 305–310
19. Duarte, M., Populo, H., Videira, A., Friedrich, T., and Schulte, U. (2002) *Biochem. J.* **364,** 833–839
20. Ingledew, W. J., and Ohnishi, T. (1980) *Biochem. J.* **186,** 111–117
21. Hellwig, P., Scheide, D., Bungert, S., Mäntele, W., and Friedrich, T. (2000) *Biochemistry* **39,** 10884–10891
22. Hanahan, D. (1983) *J. Mol. Biol.* **166,** 557–565
23. Wallace, B. J., and Young, I. G. (1977) *Biochim. Biophys. Acta* **461,** 84–100
24. Guzman, L., Belin, D., Carson, M. J., and Beckwith, J. (1995) *J. Bacteriol.* **177,** 4121–4130
25. Hellwig, P., Behr, J., Ostermeier, C., Richter, O.-M. H., Pfitzner, U., Odenwald, A., Ludwig, B., Michel, H., and Mäntele, W. (1998) *Biochemistry* **37,** 7390–7399
26. Mäntele, W. (1993) *Trends Biochem. Sci.* **18,** 197–202
27. Moss, D. A., Nabedryk, E., Breton, J., and Mäntele, W. (1990) *Eur. J. Biochem.* **187,** 565–572
28. Böttcher, B., Scheide, D., Hesterberg, M., Nagel-Steger, L., and Friedrich, T. (2002) *J. Biol. Chem.* **277,** 17970–17977
29. Friedrich, T., Hofhaus, G., Ise, W., Nehls, U., Schmitz, B., and Weiss, H. (1989) *Eur. J. Biochem.* **180,** 173–180
30. Friedrich, T., van Heek, P., Leif, H., Ohnishi, T., Forche, E., Kunze, B., Jansen, R., Trowitzsch-Kienast, W., Höfle, G. Reichenbach, H., and Weiss, H. (1994) *Eur. J. Biochem.* **219,** 691–698
31. Towbin, H., Staehlin, T., and Gordon, J. (1979) *Proc. Natl. Acad. Sci. U. S. A.* **1320,** 217–234
32. Arrondo, J. L. R., Muga, A., Castresana, J., and Goni, F. M. (1993) *Prog. Biophys. Mol. Biol.* **59,** 23–56
33. Venyaminov, S. Y., and Kalnin, N. N. (1990) *Biopolymers* **30,** 1259–1271
34. Hienerwadel, R., Boussac, A., Breton, J., Diner, B., and Berthomieu, C. (1997) *Biochemistry* **36,** 14712–14723
35. Hellwig, P., Pfitzner, U., Behr, J., Rost, B., Pesavento, R. P., Donk, W. V., Gennis, R. B., Michel, H., Ludwig, B., and Mäntele, W. (2002) *Biochemistry* **41,** 9116–9125
36. Matsushita, K., Ohnishi, T., and Kaback, H. R. (1987) *Biochemistry* **26,** 7732–7737
37. Ahlers, P. M., Zwicker, K., Kerscher, K., and Brandt, U. (2000) *J. Biol. Chem.* **275,** 23577–23582
38. Fearnley, I. M., Carrol, J., Shannon, R. J., Runswick, M. J., Walker, J. E., and

Hirst, J. (2001) *J. Biol. Chem.* **276,** 38345–38348
39. Yagi, T., Yano, T., DiBernardo, S., and Matsuno-Yagi, A. (1998) *Biochim. Biophy. Acta* **1364,** 112–125
40. Fetter, J. R., Qian, J., Shapleigh, J., Thomas, J. W., Garcia-Horsman, A., Schmidt, E., Hosler, J., Babcock, G. T., Gennis, R. B., and Ferguson-Miller, S. (1995) *Proc. Nat. l Acad. Sci. U. S. A.* **92,** 1604–1608
41. Pfitzner, U., Hoffmeier, K., Harrenga, A., Kannt, A., Michel, H., Bamberg, E., Richter, O. M., and Ludwig, B. (2000) *Biochemistry* **39,** 6756–6762
42. Puustinen, A., and Wikström, M. (1999) *Proc. Natl. Acad. Sci. U. S. A.* **96,** 35–37
43. Behr, J., Michel, H., Mäntele, W., and Hellwig, P. (2000) *Biochemistry* **39,** 1356–1363
44. Thompson, J. D., Higgins, D. G., and Gibson, T. J. (1994) *Nucleic Acids Res.* **22,** 4673–4680